EACWE2022

8th European-African Conference on Wind Engineering

20-23 September 2022 | Bucharest, Romania

Exploring stochastic dynamics and stability of an aeroelastic harvester contaminated by wind turbulence and uncertain aeroelastic loads

Luca Caracoglia[1*)]

1) Associate Professor, Northeastern University, Boston, MA 02115, USA, lucac@coe.neu.edu

ABSTRACT: The paper expands a recently developed model that examines the stochastic stability of a torsional-flutter-based harvester. The new model accounts for both uncertainty in the aeroelastic loads and wind turbulence in the incoming flow. Since the blade-airfoil is three-dimensional, three-dimensional flow effect are simulated through η_{3D}, i.e., a reduction parameter of the static lift slope, dependent on the aspect ratio of the apparatus. The first uncertainty source is a byproduct of the modelling simplifications of the aeroelastic loads, which are described by indicial function approach and ideally applicable to two-dimensional flow. The second source is the flow turbulence that operates by modifying the Parametric stochastic perturbations are applied to the parameter describing the memory-effect of the load, simulating "imperfections" in the load measurement and approximate description through η_{3D}. Stochastic flutter stability is examined by mean squares. Post-critical states are also discussed.

Keywords: wind energy, aeroelastic harvester, stochastic dynamics, output power.

1. INTRODUCTION

Wind energy technology is evolving due to the need for alternative, clean energy resources. Most applications are related to large horizontal-axis wind turbines that maximize output power. A competitive, intermediate-scale alternative is represented by simpler, wind-based energy harvesters, triggered by aeroelastic phenomena (Abdelkefi et al., 2012; Matsumoto, 2013; Pigolotti et al., 2017; Shimizu et al., 2008). These smaller dimension apparatuses have been studied by several researchers. For example, "pitch-heave" vibration of a flutter mill, equipped with porous screens to induce aeroelastic instability, has been proposed (Pigolotti, et al., 2017). Galloping-prone harvesting apparatuses, i.e., exploiting the "D" section instability, have been studied (Abdelkefi, et al., 2012) as well as vortex-induced underwater vibration of "tunable" cylindric bodies (Bernitsas et al., 2008).

Caracoglia (2018) proposed a torsional-flutter-based apparatus for extracting wind energy (Fig. 1). The apparatus exploits the leading-edge torsional flutter instability of a rigid blade-airfoil, rotating about an axis and connected through a nonlinear torsional spring mechanism. Magnetic induction of a coil system is employed for energy conversion. Various configurations can be considered with adjustable position of the rotation axis, *ab* in Figure 1: the position of the rotation axis can be moved from the leading edge ($a = -1$) to the quarter chord position ($a \approx -0.75$).

This presentation extends a recent formulation and a state-space model in the dimensionless time domain, which incorporated the effects of uncertainty in the aeroelastic loads to evaluate the dynamic stability of the apparatus. In this study, the stochastic model is generalized by also considering the effects of flow turbulence. These two sources of modeling uncertainty or randomness in the flow field may unfavorably reduce the potential for energy harvesting and, overall, the efficiency of the

*) *Corresponding author*

apparatus. The mean-square, stochastic stability problem using the equations of a state-space model. Representative numerical solutions will be discussed and analyzed.

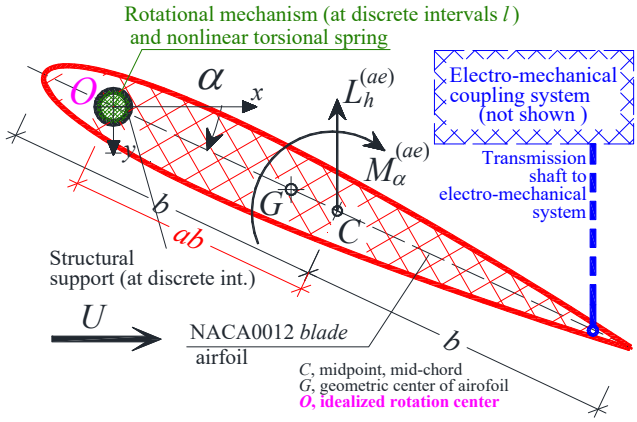

Figure 1. Schematic cross-sectional view of the proposed energy harvester.

2. MODELING BACKGROUND

2.1. Deterministic model without perturbations and flow turbulence

The linear, dynamic angular motion of the one degree of freedom (1DOF) α in Fig. 1 is:

$$\omega_\alpha^2 I_{0\alpha}\left(\frac{\mathrm{d}^2\alpha}{\mathrm{d}\tau^2}+2\zeta_\alpha\frac{\mathrm{d}\alpha}{\mathrm{d}\tau}+\alpha\right)=\pi\rho\eta_{3D}b^2U^2\ell\left\{\begin{array}{l}-k_\alpha^2\dfrac{\mathrm{d}^2\alpha}{\mathrm{d}\tau^2}\left(0.125+a^2\right)+\left(2a+1\right)C(k)\alpha\\+\left[\left(a-0.5\right)+\left(0.5-2a^2\right)C(k)\right]k_\alpha\dfrac{\mathrm{d}\alpha}{\mathrm{d}\tau}\end{array}\right\}. \quad (1)$$

The right-hand side equation is the aeroelastic torque, derived from Bisplinghoff et al. (1955) for purely rotational motion about O in Figure 1. The torque depends on the mean wind speed U parallel to the x axis; $I_{0\alpha}$ is the polar mass moment of inertia of the moving components of the apparatus; ω_α is the linear, angular frequency of the linear, spring-supported apparatus; $\tau = t\omega_\alpha$ is a dimensionless time variable; ζ_α is the damping ratio of the apparatus. The quantity $k = \omega b/U$ is a reduced angular frequency; $k_\alpha = \omega_\alpha b/U$ is the reduced angular frequency of the apparatus; $C(k) = F(k) + \mathrm{i}G(k)$ is the complex function by (Theodorsen, 1935) with $\mathrm{i}^2 = -1$. Air density is ρ. Electro-mechanical coupling will be included in Eq. (2) below.

Mean aerodynamic forces in Eq. (1) are approximately zero with average $\alpha \approx 0$. Flow turbulence is not considered in this section. Three-dimensional torque (lift) (Argentina and Mahadevan, 2005) effect is simulated by parameter $\eta_{3D} \approx \mathrm{AR}/(\mathrm{AR}+2)$; airfoil aspect ratio $\mathrm{AR} = \ell/b$ depends on the spanwise length ℓ, not shown in Figure 1. Eq. (1) can be manipulated and solved at incipient torsional flutter, i.e., by studying the vanishing of total damping (Caracoglia, 2018).

In the post-critical flutter state with $a = -1$ (leading edge rotation axis), more relevant to energy harvesting, the model is modified from Eq. (1). A state-space model is formed, composed of seven nonlinearly coupled electro-mechanical equations. Aeroelastic torque is simulated through unsteady Wagner function (Bisplinghoff, et al., 1955). The triggering mechanism depends on reduced frequency k_α, damping ratio ζ_α generalized inertia ε and cubic stiffness κ of the spring-supported rotational mechanism. The complete dynamic equation with electro-mechanical coupling is:

$$\psi_0\frac{\mathrm{d}^2\alpha}{\mathrm{d}\tau^2}+\left(\frac{1.5\varepsilon\eta_{3D}}{k_\alpha}+2\zeta_\alpha\right)\frac{\mathrm{d}\alpha}{\mathrm{d}\tau}+\left(\alpha+\kappa\alpha^3\right)=-\frac{\varepsilon\eta_{3D}}{k_\alpha^2}\left[\begin{array}{l}\Phi_0\left(\alpha+1.5k_\alpha\dfrac{\mathrm{d}\alpha}{\mathrm{d}\tau}\right)\\+1.5\left(\nu_{ae,1}+\nu_{ae,2}\right)+\mu_{ae,1}+\mu_{ae,2}\end{array}\right]-\Psi\iota\,, \quad (2)$$

with $\psi_0 = (1 + 9/8\varepsilon\eta_{3D})$; $\Psi = 4b^2(\Phi_{\mathrm{e.m.c.}})^2/(\omega_\alpha I_{0\alpha} R_C)$ is a dimensionless electro-mechanical coupling with eddy-current power circuit, with $\lambda_{RL} = R_C/(\omega_\alpha L_C)$ a generalized impedance of the power

circuit with R_C resistance (ohms) and L_C inductance (henries). On the right-hand side of Eq. (2), $\iota(\tau)$ is a normalized output current; $\nu_{ae,1}$, $\nu_{ae,2}$, $\mu_{ae,1}$ and $\mu_{ae,2}$ are aeroelastic states and $\Phi_0 = 0.5$.

2.2. Stochastic model with inflow turbulence and aeroelastic load perturbations

First, Along-wind turbulence $u(\tau)$ is simulated as a zero-mean, Gaussian white noise, fully correlated over the surface of the apparatus. This hypothesis is compatible with the observation that atmospheric turbulence length scales are considerably larger than the characteristic length of the apparatus $\sqrt{b^2+\ell^2} = b\sqrt{1+\mathrm{AR}^2} \approx 10b$ (even for large $\mathrm{AR} = 10$). The Gaussian process parametrically modifies the constant flow speed term U^2 in Eq. (1) to $(U+u(\tau))^2 \approx U^2[1+2\hat{u}(\tau)]$ with normalized $\hat{u} = u/U$, i.e., the noise is multiplicative with standard deviation $\sigma_{\hat{u}}$ equal to the flow turbulence intensity.

Second, aeroelastic load modeling errors are simulated using the Jones (1939) formulation of the Wagner function and the aeroelastic states defined in Eq. (2). The format of the dynamic equations describing the two aeroelastic states $\nu_{ae,2}(\tau)$ and $\mu_{ae,2}(\tau)$ that are randomly perturbed, is:

$$\frac{\mathrm{d}\nu_{ae,2}}{\mathrm{d}\tau} = \left(\bar{d}_2 + \Delta_{d2}(\tau)\right)\left[c_2\frac{\mathrm{d}\alpha}{\mathrm{d}\tau} - k_\alpha^{-1}\nu_{ae,2}\right], \quad \frac{\mathrm{d}\mu_{ae,2}}{\mathrm{d}\tau} = k_\alpha^{-1}\left(\bar{d}_2 + \Delta_{d2}(\tau)\right)\left(c_2\alpha - \mu_{ae,2}\right), \quad \text{(3a, 3b)}$$

where the parameter $\Delta_{d2}(\tau)$ is another zero-mean, white noise of pre-assigned standard deviation σ_{d2}, whereas the noise-free reference or constant mean value is $\bar{d}_2 = 0.3$. By contrast, the two remaining states, $\nu_{ae,1}(\tau)$ and $\mu_{ae,1}(\tau)$, are unaffected. Noting that the same random load variation $\Delta_{d2}(\tau)$ is applied to both Eqs. (3a-3b) above as a second multiplicative noise, the resultant system of differential equations is parametric, enabling both incipient and post-critical operational analyses.

A system of stochastic differential equations (Grigoriu, 2002) is derived as a function of two scalar, independent unit Wiener noises $B_{\hat{u}}(\tau)$ (from $\hat{u}$) and $B_{\Delta 2}(\tau)$ (from Δ_{d2}) and vector

$$\mathbf{W}_{\mathrm{em}}(\tau) = \left[\alpha(\tau), \mathrm{d}\alpha/\mathrm{d}\tau, \nu_{ae,1}(\tau), \nu_{ae,2}(\tau), \mu_{ae,1}(\tau), \mu_{ae,2}(\tau), \iota(\tau)\right]^T = \left[W_{\mathrm{em},1}, \dots, W_{\mathrm{em},7}\right]^T. \quad (4)$$

The final Itô-type equation depends on a nonlinear (NL) drift $\mathbf{q}_{\mathrm{NL},\Delta}$ function, a linear (L) diffusion matrix $\mathbf{Q}_{\mathrm{L},\Delta 2}$ that specifically depends on the "unit aeroelastic Wiener error" $B_{\Delta 2}(\tau)$ (rescaled to account for standard deviation σ_{d2}), and a nonlinear diffusion functional $\mathbf{\Theta}_{\mathrm{NL},\hat{u}}(\mathbf{W}_{\mathrm{em}}; \sigma_{\hat{u}})$, which is applied to "unit Wiener turbulence" $B_{\hat{u}}(\tau)$ and depends on the standard deviation $\sigma_{\hat{u}}$. This equation is:

$$\mathrm{d}\mathbf{W}_{\mathrm{em}} = \mathbf{q}_{\mathrm{NL}}(\mathbf{W}_{\mathrm{em}}; \sigma_{\hat{u}}, \sigma_{d2})\mathrm{d}\tau + \sqrt{2\pi}\mathbf{Q}_{\mathrm{L},\Delta 2}\mathbf{W}_{\mathrm{em}}\mathrm{d}B_{\Delta 2}(\tau) + 2\mathbf{\Theta}_{\mathrm{NL},\hat{u}}(\mathbf{W}_{\mathrm{em}}; \sigma_{\hat{u}})\mathrm{d}B_{\hat{u}}(\tau). \quad (5)$$

The non-zero elements of the 7-by-7 matrix $\mathbf{Q}_{L,\Delta 2}$ are exclusively three, i.e.,

$$\left(\mathbf{Q}_{\mathrm{L},\Delta}\right)_{4,2} = \left(\mathbf{Q}_{\mathrm{L},\Delta}\right)_{6,1} = \sigma_{d2}k_\alpha^{-1}c_2, \quad \left(\mathbf{Q}_{\mathrm{L},\Delta}\right)_{6,6} = -\sigma_{d2}k_\alpha^{-1}, \quad \text{(6a, 6b)}$$

In Eq. (5) the Wong and Zakai (1965) correction terms have been included. Mean – square stability is examined using second moment (largest) Lyapunov exponent of a "relevant dynamics" sub-vector of the system, i.e., $\mathbf{\Xi}(\tau) = [\alpha, \mathrm{d}\alpha/d\tau]^T = [W_{\mathrm{em},1}, W_{\mathrm{em},2}]^T$. The stability varies as a function of mean wind speed U or k_α. This approach enables evaluation of both incipient and post-critical flutter, i.e., the output current $\iota = w_{\mathrm{em},7}$ and energy conversion. The second moment Lyapunov exponent $\Lambda_{\mathbf{\Xi}}(2)$ is evaluated by Monte Carlo sampling. The realizations of Eq. (5) are solved by Euler numerical integration (Kloeden et al., 1994), from which the exponent is approximated as $\Lambda_{\mathbf{\Xi}}(2) \approx \log\left(\mathrm{E}\left[\left\|\mathbf{\Xi}(\tau_j)\right\|^2\right]\right)/\tau_j$ with discrete time τ_j and time index j sufficiently large (infinity). Monte

3. PRELIMINARY RESULTS, DICUSSION AND CONCLUSIONS

Numerical solution of the stochastic model in a post-critical state is considered. The reference quantities are set as follows: electro-mechanical coupling $\Psi = 0.01$, generalized impedance $\lambda_{RL} = 0.75$, $\mathrm{AR} = 4$ and $\kappa = 100$ in dimensionless units. Three basic configurations are investigated: Type 0 with $\omega_\alpha/2\pi$=0.25 Hz, b=0.25 m, $I_{0\alpha}/\ell$=20 kg-m^2/m, Type 1 with $\omega_\alpha/2\pi$=0.20 Hz, b=0.25 m, $I_{0\alpha}/\ell$=40 kg-m^2/m; Type 2 with $\omega_\alpha/2\pi$=0.10 Hz, b=0.50 m, $I_{0\alpha}/\ell$=300 kg-m^2/m.

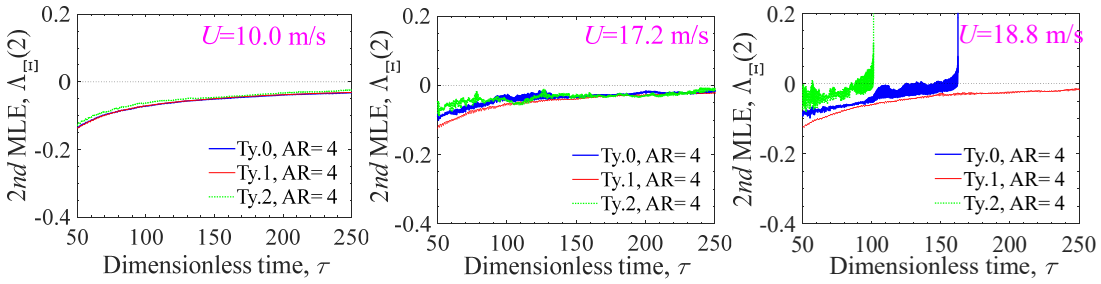

Figure 2. Second Moment Lyapunov Exponent (MLE) $\Lambda_{\Xi}(2)$, at various flow speeds U, for Type-0, Type-1 and Type-2 apparatus - random aeroelastic load with mean value $\bar{d}_2 = 0.3$ and standard deviation $\sigma_{d2} = 0.07$; negligible turbulence $\sigma_{\hat{u}} \approx 0$.

Fig. 2 summarizes an example of stochastic stability analysis at various mean flow speeds U for random aeroelastic load with mean value $\bar{d}_2 = 0.3$ and standard deviation $\sigma_{d2} = 0.07$. At this time, the effect of flow turbulence is neglected $\sigma_{\hat{u}} \approx 0$. The figure panels reveal the predominantly stable condition of Type-1 apparatus, i.e., inefficient from the point of view of harvesting, with Lyapunov exponent $\Lambda_{\Xi}(2) < 0$. On the contrary the right panel shows the departure from a stable configuration for the other two types at $U = 18.8$ m/s. Type-2 apparatus also exhibits incipient instability at a lower flow speed (center panel) with $\Lambda_{\Xi}(2)$ crossing the zero axis. The figure demonstrates that the proposed numerical solution approach is adequate for the purpose of stability analysis. Further evidence will be presented to examine the combined effect of both flow turbulence and randomly perturbed aeroelastic load, as well as the performance of the apparatus in terms of output current.

Acknowledgements

This material is based in part upon work supported by the National Science Foundation (NSF) of the United States of America, Award CMMI-2020063. Any opinions, findings and conclusions or recommendations are those of the author and do not necessarily reflect the views of the NSF.

References

Abdelkefi A, Nayfeh AH, Hajj MR (2012). Design of piezoaeroelastic energy harvesters. Nonlinear Dynamics 68, 4: 519-530.

Argentina M, Mahadevan L (2005). Fluid-flow-induced flutter of a flag. PNAS - Proceedings of the National Academy of Sciences of the United States of America 102, 6: 1829-1834.

Bernitsas MM, Raghavan K, Ben-Simon Y, Garcia EMH (2008). VIVACE (Vortex Induced Vibration Aquatic Clean Energy): A new concept in generation of clean and renewable energy from fluid flow. Journal of Offshore Mechanics and Arctic Engineering 130, 4: 041101.

Bisplinghoff RL, Ashley H, Halfman RL (1955). Aeroelasticity. Dover Publications Inc., Mineola, NY, USA.

Caracoglia L (2018). Modeling the coupled electro-mechanical response of a torsional-flutter-based wind harvester with a focus on energy efficiency examination. Journal of Wind Engineering and Industrial Aerodynamics 174: 437-450.

Grigoriu M (2002). Stochastic calculus. Applications in science and engineering. Birkhäuser, Boston, MA, USA.

Jones RT (1939). The unsteady lift of a finite wing. NACA, Technical Note 682.

Kloeden PE, Platen E, Schurz H (1994). Numerical solution of stochastic differential equations through computer experiments. Springer-Verlag, Berlin-Heidelberg, Germany.

Matsumoto M (2013). Flutter and its application - Flutter mode and ship navigation. Journal of Wind Engineering and Industrial Aerodynamics 122: 10-20.

Pigolotti L, Mannini C, Bartoli G, Thiele K (2017). Critical and post-critical behaviour of two-degree-of-freedom flutter-based generators. Journal of Sound and Vibration 404: 116-140.

Shimizu E, Isogai K, Obayashi S (2008). Multiobjective design study of a flapping wind power generator. Journal of Fluids Engineering, ASME 130, 2: 021104.

Theodorsen T (1935). General theory of aerodynamic instability and the mechanism of flutter. National Advisory Committee for Aeronautics, Technical Report 496.

Wong E, Zakai M (1965). On the relation between ordinary and stochastic differential equations. International Journal of Engineering Science 3: 213-229.